ARMY RESEARCH LABORATORY

Detection of Bioaerosols using Single Particle Thermal Emission Spectroscopy (First-year Report)

by Dr. Kristan P. Gurton, Melvin Felton, and Dr. Yongle Pan

ARL-TR-5934 **February 2012**

NOTICES

Disclaimers

The findings in this report are not to be construed as an official Department of the Army position unless so designated by other authorized documents.

Citation of manufacturer's or trade names does not constitute an official endorsement or approval of the use thereof.

Destroy this report when it is no longer needed. Do not return it to the originator.

Army Research Laboratory
Adelphi, MD 20783-1197

ARL-TR-5934 **February 2012**

Detection of Bioaerosols using Single Particle Thermal Emission Spectroscopy (First-year Report)

Dr. Kristan P. Gurton, Melvin Felton, and Dr. Yongle Pan
Computational and Information Sciences Directorate, ARL

REPORT DOCUMENTATION PAGE

Form Approved
OMB No. 0704-0188

1. REPORT DATE *(DD-MM-YYYY)*	2. REPORT TYPE	3. DATES COVERED (From - To)
February 2012	DRI	October 2010 to October 2011

4. TITLE AND SUBTITLE
Detection of Bioaerosols using Single Particle Thermal Emission Spectroscopy (First-year Report)

5a. CONTRACT NUMBER

5b. GRANT NUMBER

5c. PROGRAM ELEMENT NUMBER

6. AUTHOR(S)
Dr. Kristan P. Gurton, Melvin Felton, and Dr. Yongle Pan

5d. PROJECT NUMBER

5e. TASK NUMBER

5f. WORK UNIT NUMBER

7. PERFORMING ORGANIZATION NAME(S) AND ADDRESS(ES)
U.S. Army Research Laboratory
ATTN: RDRL-CIE-S
2800 Powder Mill Road
Adelphi, MD 20783-1197

8. PERFORMING ORGANIZATION REPORT NUMBER
ARL-TR-5934

9. SPONSORING/MONITORING AGENCY NAME(S) AND ADDRESS(ES)

10. SPONSOR/MONITOR'S ACRONYM(S)

11. SPONSOR/MONITOR'S REPORT NUMBER(S)

12. DISTRIBUTION/AVAILABILITY STATEMENT
Approved for public release; distribution unlimited.

13. SUPPLEMENTARY NOTES

14. ABSTRACT
We are investigating a new type of single aerosol particle spectroscopy that is designed to identify unique and identifiable characteristic features in measured molecular emission/absorption spectra in the thermal infrared (IR) region from 3 to 12 μm. Our objective is to improve the ability to identify and distinguish mundane bioaerosols from more toxic varieties and/or species. During year 1 of a two-year study, we developed and investigated various techniques required for single bioparticle generation, transfer, and manipulation. During the second year, our goal will be to directly measure in situ the gray-body spectral emission from a 1–20 micron size bioparticle that is optically heated to temperatures of approximately 100–300 °C above ambient temperatures. The resultant thermal emission is dispersively resolved using 190-mm Horiba spectrometer that houses a time-gated 32-element mercury cadmium telluride (MCT) linear array. In this report, we outline the fundamental theory for our approach, discuss in detail the various single particle transport and trapping methods required to conduct single particle thermal emission spectroscopy (SPTES) in situ, and present the result that we photophoretically trapped weak absorbing bioaerosol particles by laser bottle beam via optical aberration.

15. SUBJECT TERMS
Chem bio detection, single particle, emission spectroscopy

16. SECURITY CLASSIFICATION OF:			17. LIMITATION OF ABSTRACT	18. NUMBER OF PAGES	19a. NAME OF RESPONSIBLE PERSON
a. REPORT	b. ABSTRACT	c. THIS PAGE			Kristan Gurton
Unclassified	Unclassified	Unclassified	UU	20	19b. TELEPHONE NUMBER (*Include area code*) (301) 394-2093

Standard Form 298 (Rev. 8/98)
Prescribed by ANSI Std. Z39.18

Contents

List of Figures

1. Introduction

The primary goal for this proposed research is to develop a novel optical technique that is capable of detecting the presence of harmful biological aerosol particles at ambient concentrations. Currently, there are no reliable means for accurate "real-time" detection and identification of hazardous biological aerosols. Early warning systems are badly needed that are capable of *instantaneously* detecting the presence of airborne biological warfare (BW) agents. Existing point-detection methods typically involve fluorescent antibody tagging and other biochemical methodologies require long periods of time to process and analyze. Such systems also require an a priori "guess" as to what specific antibodies should be considered. As a result, such biochemical specific systems are easily thwarted by choosing a slightly atypical agent or variant species.

If the rapid detection and identification of BW agents is a primary objective, then direct *optical* probing must be considered. Various promising methods that rely on inelastic phenomena induced by laser radiation include Raman scattering, plasma emission, fluorescent emission, and thermal emission (*1–7*). However, Raman, plasma emission, and fluorescent emission are strongly affected by subtle changes in many chemical and physical parameters that make reliable deployment in real-time application extremely difficult, e.g., molecular-chemical structure, interactions between adjacent molecules, internal distribution of refractive indices, and particle shape. In addition, they also depend on the parameters of the excitation laser, i.e., intensity wavelength and incident direction (*8, 9*). In contrast, the measured thermal emission from a single particle depends solely on two physical parameters: temperature and emission cross section (*10–12*). Equation 1 shows the spectral intensity, δI_λ, emitted by a unit area of particle surface,

$$\delta I_\lambda = \varepsilon(\lambda) R_b(\lambda, T_p), \tag{1}$$

where $\varepsilon(\lambda)$ is the particle spectral emissivity cross section and $R_b(\lambda, T_p)$ is the Planck function, i.e., the radiance of a blackbody at temperature T_p.*

According to the generalized Kirchhoff's law, the emission cross section of the thermal radiation for an arbitrary object, for a given wavelength, polarization, and direction, is equivalent to the absorption cross section at the same wavelength and polarization state, except the direction of the flux is reversed.† Van de Hulst and Bohren extend the Kirchhoff relationship to small aerosol particles and state that the measurement of the emission cross section, $\varepsilon(\lambda)$ yields the same

*In general, the emissivity is a function of wavelength, direction, and temperature, but for the case at hand we assume modest temperatures, well below ionization, and that the radiance is captured over a sufficiently large enough solid angle so as to reduce directional variation.

†One of the most thorough description involving the often misused derivation of Kirchhoff's law can be found in Hottel, H. C.; Sarofim, A. F. *Radiative Transfer*; McGraw Hill: New York, 1967, pp. 4–24.

microphysical properties for small arbitrarily shaped particles as the absorption cross section, $\alpha(\lambda)$ (*13, 14*). However, as pointed out by Bohren, Hottel et al., the assertion that the thermal system(s) must be in thermal equilibrium for Kirchhoff's law to be valid is not entirely true, and as a result, the Kirchhoff's relations are still valid for non-equilibrium so long as they are best characterized as behaving like a gray-body system. Hottel states for a gray-bodies (emissivity less than 1), Kirchhoff's analysis, which relates the spectral emissivity to spectral absorptivity, is still valid even if the body is not in thermal equilibrium so long as the absorption cross section is not affected by changes in temperature of the radiation source.

Nonetheless, it is not our immediate goal to *quantitatively* measure the absorption spectra via the measured emission (although there appears a theoretical basis for doing so), we merely assert that unique absorption features inherent in complex bio-*molecular* materials/particles will be present in corresponding emission spectra when *measured in the thermal IR*, i.e., approximately 3–12 μm. Additional, we intend to show that these features inherent in the spectra will be highly reproducible regardless of changes in particle size or shape.

Additional information about the structural nature of the particle can be deduced by considering the rate at which the particle dissipates its thermal energy. A measurement of the so-called "characteristic cooling time," τ, refers to the time required for particle heat transfer to the surrounding gas. It is well known that for a given size particle, the rate at which the particle cools is a measure of whether the structure is solid, liquid, or amorphous (*15, 16*).

Let's consider possible mechanisms involved for particle cooling after it has been heated to some temperature, $T_{p,}$ above the surrounding gas temperature, T_g, where $T_p > T_g$. There are three processes that cause cooling of the particle: (1) heat transfer to the surrounding gas, (2) heat energy lost due to radiation, and (3) particle evaporation. The total heat flux from the particle in the free molecular regime is

$$\dot{q} = 4\pi a^2 \frac{1}{2} p_g c_t \left(\frac{T_p}{T_g} - 1\right) + 4\pi a^2 \varepsilon\sigma\left({T_p}^4 - {T_g}^4\right) + 4\pi a^2 G_v \Delta h, \tag{2}$$

$$c_t = \sqrt{\frac{8kT_g}{\pi m_g}} \quad , \tag{3}$$

where $p_g$is the gas pressure, m_g and c_t are the mass and average velocity of the gas molecule, ε is the total particle emissivity, k and σ are Boltzmann and Stefan-Boltzmann constants, G_v is the flux density of vapor leaving the particle, and Δh is the specific heat of evaporation. The first term on the right-hand side of equation 2 represents the heat of conductivity in a free-molecular regime with the assumption of diffuse reflection of gas molecules at the particle surface (*17*). The second and third terms represent heat loss due to radiation and evaporation, respectively, and are assumed small so long as the particle heating is kept moderate and we consider the bioparticle to be particulate in nature (a condition that can be relaxed later).

We now consider a typical energy balance equation for the cooling cycle of a particle after the heat source is removed. The rate at which the particle cools is given by

$$m_p c_p \frac{dT_p}{dt} = -\dot{q} \ , \tag{4}$$

where T_p is the instantaneous temperature of the particle, m_p is the mass of the particle, and c_p is the specific heat of the particle. Combining equations 4 and 2 and integrating over time, t, we find the solution corresponding to particle temperature $T_p(t)$ of the form

$$\frac{T_p - T_g}{T_g} = \left(\frac{T_p^0}{T_g} - 1\right) exp^{\left(-\frac{t}{\tau}\right)} \ , \tag{5}$$

where T_p^0 is the initial temperature at t = 0, and the reservoir of surrounding gas is assumed large enough so that T_g remains constant. The parameter τ is taken to be the characteristic cooling period for the particle due to heat transfer to the surrounding gas. To get an order of magnitude for anticipated values of τ, we consider a glycerin particle of varying diameters, with the following physical parameters: mass-density, $\rho_p = 1.27$ (kg/m3); thermal conductivity, K = 0.29 (W/mK); and a specific heat value of c_p = 2.43 (kJ/kg*K).

Fourier heat-conduction calculations are conducted in which the characteristic cooling period is plotted as a function of particle radius based on the final condition, $\frac{T_p - T_g}{T_g} = 0.90$, i.e., the particle has cooled to within 10% of the ambient surrounding gas temperature (figure 1) (*18*).

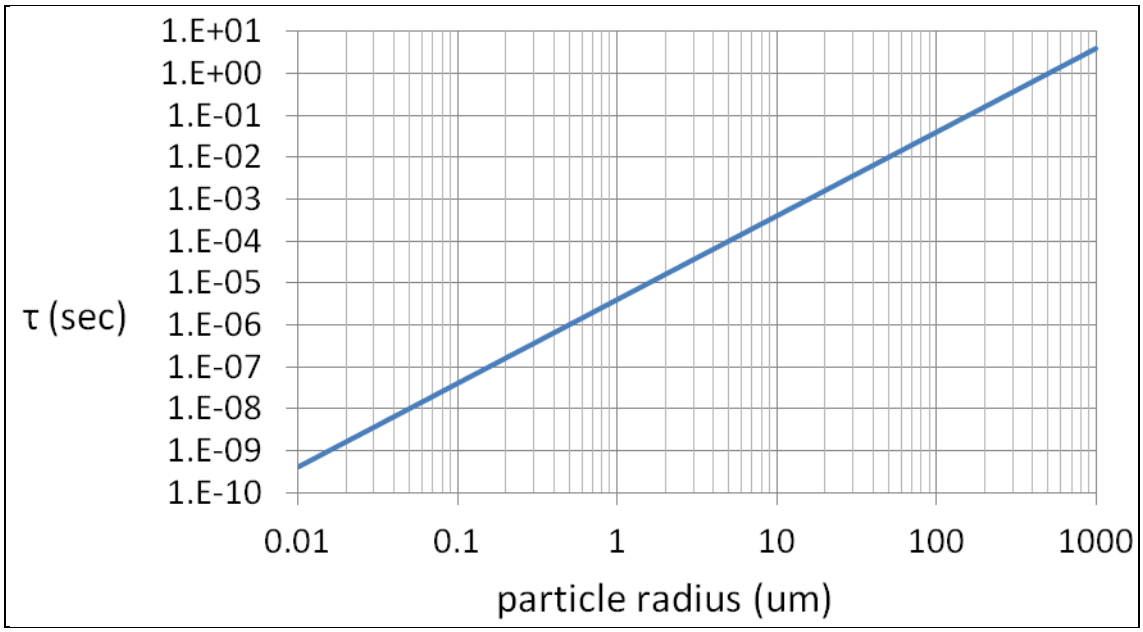

Figure 1. Plot of the characteristic cooling period, τ (seconds), for a spherical glycerin particle heated to some initial temperature T_p, and T_g is the temperature of the surrounding gas, where τ has been calculated for the condition $\frac{T_p - T_g}{T_g} = 0.90$.

The anticipated range of diameters for our study are expected to be between 1–30 μm. Based on the results calculated for glycerin shown in figure 1 (considered conservative since the thermal conduction coefficient for particulates are much higher), the anticipated characteristic cooling periods will range from approximately 1.0 μs to 10.0 ms. Minimum integration (and readout) periods for the time-gated 32-element mercury cadmium telluride (MCT) linear array are 10 μs. Based on these parameters, we anticipate being able to temporally resolve multiple spectra as the particle cools, resulting in a direct measure of τ. From these values, we hope to infer additional "structural" information about the particle. It is our hope that when coupled with corresponding measured absorption/emission IR spectra, this novel/new information set will improve the ability to detect, distinguish, and identify harmful toxic bioaerosols at trace levels.

2. Experiment

A simple schematic highlighting key components necessary for conducting single particle thermal emission spectroscopy (SPTES) is shown in figure 2. The diagram shows a conventional "dynamic" free-flowing particle delivery system similar to that described by Pan et al. (*5*). In figure 2, test particles are transported and focused to a sample volume (~300 μm in diameter) using a flow cytometry arrangement. This consists of two isokinetically matched nozzles, one for focusing the particle into the sample region and one to capture/collect the particles after optical probing has occurred (*19*). In order to properly gate and trigger the heating laser pulse and subsequent emission capture, two intersecting diode lasers (operating at 635 and 780 nm) are used to define a trigger volume along the particle's trajectory. Once the particle has exited the focal nozzle, it enters the trigger volume and scattered light is detected using a set of band-filtered Hamamatsu miniature photo-multiplier tubes (PMTs). Only when the particle is in the correct location will both beams simultaneously trigger the probe laser (used for heating), and after some pre-determined delay, the time-gate for spectrometer signal integration is turned on. At the current flow rate of 0.8 liter/min, we estimate a signal integration time to be on the order of 10–20 μs. Our goal is to slow this rate down to 0.1 liter/min (without losing particle position accuracy) in order to increase integration period(s) to the 1.0 m/s range.

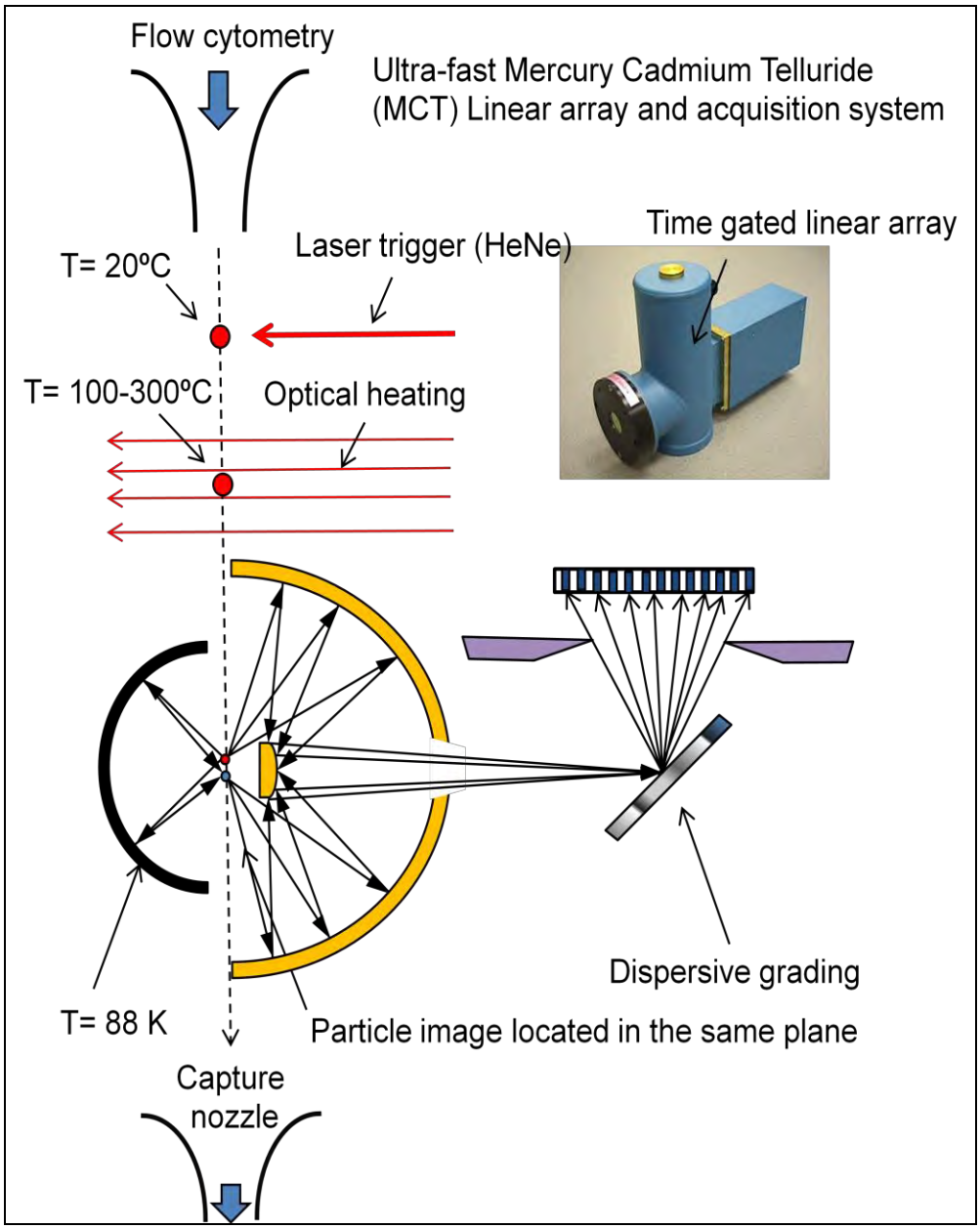

Figure 2. Simple schematic showing the particle delivery system, triggering lasers, heating laser and capture optics/spectrometer required for SPTES.

In order to generate sufficient levels of thermal emission, we expect to heat the particulate bioparticles to temperatures in roughly the 200–300 °C range. To accomplish this, the output from a pulsed, 1.06-µm neodymium-doped yttrium aluminum garnet (Nd:YAG) laser is used to illuminate the test particle. Laser intensity are greatly attenuated to ensure that heat rates are kept to a minimum to ensure that the particle remains intact and does not undergo any form of meaningful phase change.

The resultant thermal radiance is captured using a highly efficient gold-coated Schwarzschild objective with a numeric aperture (NA) of 0.50. The broadband thermal radiance is focused into 190-mm Horiba spectrometer where the radiance is dispersed onto an ultrafast, time-gated, liquid nitrogen (LN2) cooled 32-element MCT linear array. Spectral selection within the 3–12 μm waveband is accomplished using a three-grating turret that rotates a user-specified grating at the focal spot of the objective.

Two radiometric "tricks" will be incorporated to maximize signal to noise (S/N). First, a spherical concave mirror will be positioned so the hot particle is effectively imaged twice (figure 2). It is well known that that by properly positioning a spherical mirror slightly off-axis with respect to a point-source, the apparent intensity is nearly doubled by the return of the backward-propagating rays. Second, the background that the particle is imaged against will appear to be at a NL2 temperature of 88 K, thus greatly reducing the ambient noise levels. This is accomplished by projecting the image of the NL2-cooled MCT linear array back through the system and reimaging it at the particle via the spherical mirror, i.e., using the Narcissus effect inherent in cooled imaging systems as an actual cold source. To date, all of the previously described systems have been acquired, assembled, and tested, except for the Horiba spectrometer, which is due to delays in funding/procurement and technical issues encountered by the vendor involving the proprietary design of the ultra-fast data acquisition (DAQ) electronics.

3. Particle Trapping

Typical particle velocities in a free flowing arrangement as shown in figure 2 are predicted to be on the order of 10 m/s as the particles exit the focusing nozzle (*20*). Based on a field of view (FOV) defined by the Schwarzschild objective of 500 μm, we predict a maximum integration period of $\Delta t = 50$ ms. As stated earlier, our goal is to reduce particle velocities to levels below 1 m/s (without losing the ability to focus the particle stream), resulting in a factor of 10 increase in the detector integration period. However, since the expected power emitted by a small micron-sized particle is expected to be in the nW range, it would be advantageous to allow the MCT linear array to integrate on the radiant signal for as long as possible in order to establish our initial "proof-of-concept."‡ Such a technique must allow for stable trapping and manipulation of small uncharged bioparticles in the size range 1–20 μm.

To accomplish this task by capturing and trapping small particles in free-space, several acoustic and optical techniques were examined, i.e., methods that rely on acoustic levitation, radiative pressure, and suspension of small particles using the photophoretic force (*21–23*). Experiments

‡Preliminary calculation based on conservative assumptions show that a 10-μm moderately absorbing particle heated to 100 °C will emit 80 nW into 3 steradians (expected collection efficiency). Using a single element LN2-cooled MCT detector with a noise equivalent power (NEP) of 7x10(–13) W/Hz, yields a detection S/N > 13 (assuming a sufficiently cooled background). We consider this a worst-case scenario and intend to optimize the system for substantially higher S/N.

showed that acoustic levitation was limited to macro-particles with diameters >100 μm with limited optical access, and techniques involving radiative pressure were relatively weak when compared to trapping using photophoretics. Results in our laboratory showed the photophoretic force method to be several orders of magnitude greater than the radiative force technique pioneered by Ashkin et al. (*22*).

Photophoretic trapping occurs when a moderately absorbing particle is positioned within a null field intensity region of a focused laser, i.e., a small volume in which the optical intensity is a minimum surrounded by regions of high light intensity. Given these conditions, as a particle migrates towards a region of high intensity region that bounds the void region, optical absorption occurs resulting in non-uniform particle heating. Kinetic energy is transferred from surrounding gas molecules to the particle, exerting a net force away from the high intensity region thus forcing it back into a low intensity region. The particle is effectively trapped when the dimensions of the void and particle are approximately the same. Recently, since 2009, there are several methods in the literature describing how to generate laser-induced null fields appropriate for photophoretic trapping, some more complex than others, e.g., bottle-beam trapping, vortex beam trapping, and Bessel beam trapping (*24–26*).

After a thorough review of the various methods designed to produce photophoretic trapping, we realized that the simplest means for generating these so-called null field points occur every time one attempts to focus a laser with an uncorrected spherical lens, i.e., common spherical aberration occurs near the focal region. When parallel rays aligned with the optical axis are focused using a common spherical lens, marginal rays (rays near the edges of the lens) focus at a slightly different point on the optical axis than rays that enter near the lens center (figure 3a, bottom). This results in “hot” and “cold” points along the optical axis in which a particle can be trapped. Initially, we were able to easily trap agglomerated carbon black particles using the output of a focused 5-mW helium-neon (HeNe) laser, but were unable to trap less absorbing biological-type particles. Because bio-materials are strong absorbers in the mid-IR, we attempted trapping with 1.064- and 10.6-μm laser systems, but had little success.

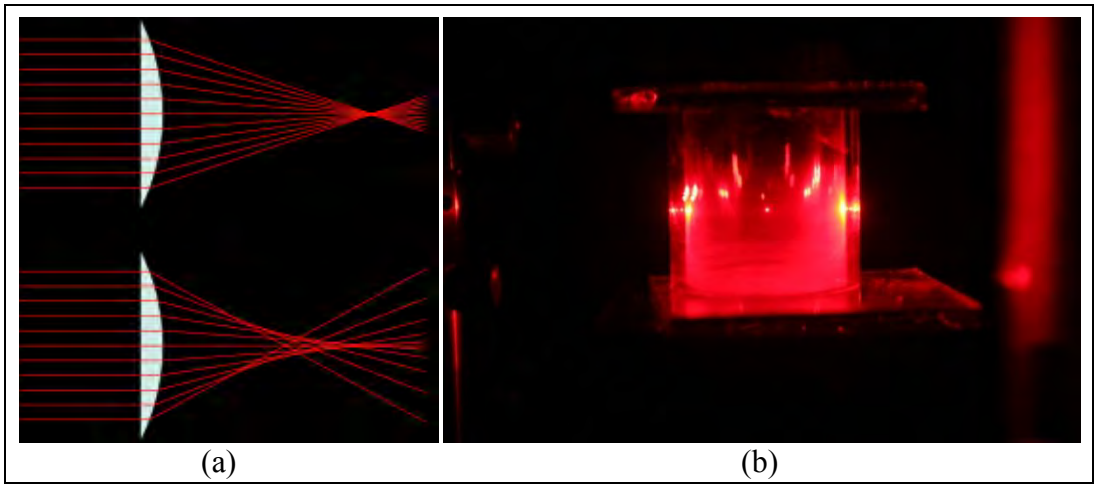

Figure 3. (a) A well-defined focal spot for a spherically "corrected" lens (top) and the resultant trapping region(s) located along the optical axis that occurs when an uncorrected spherical lens is used to focus a laser beam, i.e., spherical aberration occurs (bottom). (b) A photograph of a 15-μm diameter stably trapped *bacillus subtilis* (BG) endospores using photophoretic force generated by a focused 50-mW HeNe laser.

After many failed attempts working in the IR, we went back to using the visible HeNe laser operating at 632.8 nm with which we had so much initial success. However, this time we observed a single, fairly unstable, at first, BG endospore agglomerate (maybe 5–6 μm in diameter) being trapped in a void region near the focal point of a plano-convex lens. As we observed the particle motion, we noticed that very small, single, 1-μm endospore particles were being propelled into the agglomerate via radiative pressures along the beam. The trapped agglomerate grew in size until it matched the void dimensions, resulting in a stably trapped bio-particle (figure 3b).

Our initial assumptions, which proved to be incorrect, were that the particle needed to be *strongly* absorbing at the particular laser wavelength. All prior studies describing success with photophoretic trapping used carbon-based particles, which are extremely strong absorbers in the visible and IR. This assumption proved to be incorrect. After further study, we concluded that weak to moderately absorbing particles could be stably trapped using the photophoretic technique; however, the following must apply: (1) the particle must have relatively low thermal diffusivity (which an agglomerate will exhibit) so that asymmetric particle heating can occur, and (2) the dimensions of the particle must match that of the created optical void(s).

4. Conclusion

In this preliminary report (year 1 of a two-year study), we describe the theoretical basis for measuring in situ emission spectra in the thermal IR region emitted by a single, optically heated bioaerosol particle. We believe that such spectra will offer additional information about the

biochemical composition and nature of the particle. As a result, such a study will improve the ability of Department of Defense (DoD) and civilian scientists to develop new point detection sensors capable of detecting the presence of toxic bioaerosols at ambient concentrations.

We identify two key advantages for considering SPTES. First, by spectrally resolving the emission over a continuum in the mid-IR, intrinsic molecular characteristics that result from vibration, translation, and rotation transitions become apparent, thus producing a more definitive method for distinguishing, identifying, and/or classifying bioaerosols. Second, because SPTES does not rely on elastic or inelastic scattering, it is unaffected by the nature in which the particle is heated and, as a result, the emission spectra will be far less sensitive to changes in particle shape and/or size. This should result in a greater degree reliably and reduced false-alarm rates that plague current systems when "real-time" aerosol samples are considered (*27*).

Much of our experimental focus during the first year has involved developing particle generation, capture, and delivery systems. We have developed both free-flowing and static particle positioning systems required for SPTES. Although there are many accounts documenting photophoretic particle trapping of carbon-related materials, we believe we are the first group to successfully trap and manipulate a moderately weakly absorbing bioparticle using simple spherical aberration.

During year 2, we intend to take delivery of a high-speed dispersive spectrometer and incorporate it into both our static and dynamic particle delivery systems, to measure, for the first time, the spectral emission and absorption from an optically heated aerosols particle in the spectroscopically rich region of the thermal IR.

5. References

1. Pan, Yong-Le; Hill, Steven C.; Coleman, Mark. Photophoretic Trapping of Absorbing Particles in Air: Measurement of their Single-particle Raman Spectra. *Phys Rev. Lett.* **Nov. 2011**.

2. Windom, B. C.; Diwakar, P. K.; Hahn, D. W. Dual-pulse Laser Induced Breakdown Spectroscopy for Analysis of Gaseous and Aerosol Systems: Plasma-analyte Interactions. *Spectrochimica Acta Part B: Atomic Spectroscopy* **July 2006**, *61* (7), 788–796.

3. Hahn, D. W.; Lunden, M. M. Detection and Analysis of Particles by Laser-induced Breakdown Spectroscopy. *Aerosol Sci. and Tech.* **2000**, *33* (1), 30–48.

4. Kaye, P.; Stanley, W.; Hirst, E.; Foot, E. Single Particle Multichannel Bio-aerosol Fluorescence Sensor. *Optics Exp.* **2005**, *13* (10), 3583–3593.

5. Pan, Yong-Le; Hill, S.; Pinnick, R.; House, J.; Flagan, R.; Chang, R. Dual-excitation-wavelength Fluorescence and Elastic Scattering for Differentiation of Single Airborne Pollen and Fungal Particles. *Atmos. Envoi.* **2011**, *45*, 1555-1563.

6. Kaye, P.; Stanley, W.; Hirst, E.; Foot, E. Single Particle Multichannel Bio-aerosol Fluorescence Sensor. *Optics Exp.* **2005**, *13* (10), 3583–3593.

7. Hairston, P. P.; Ho, J. Design of an Instrument for Real-time Detection of Bioaerosols using Simultaneous Measurement of Particle Aerodynamic Size and Intrinsic Fluorescence. *J. Aerosol Sci.* **1997**, *28*, 471–482.

8. Boutou, V.; Favre, C.; Hill, S. C.; Pan, Y. L.; Chang, R. K.; Wolf, J. P. Backward Enhanced Emission from Multiphoton Processes in Aerosols. *Appl. Phys. B* **2002**, *75*, 145–152.

9. Weigel, T.; Shulte, J.; Schweiger, G. Inelastic Scattering by Particles of Arbitrary Shape. *J. Opt. Soc. Am. A* **2006**, *23*, 2797–2802.

10. Rytov, S. The Theory of Electrical Fluctuations and Thermal Radiation, (English Translation by US Air Force Cambridge Research Center, Bedford, MA, Rep. AFCRC-TR-59-162). USSR Academy of Science, Moscow, 1953.

11. Bekefi, G. *Radiation Processes in Plasmas*; John Wiley & Sons: New York, 1966.

12. Moteki, N.; Kondo, Y.; Takegawa, N.; Nakamura, S. Directional Dependence of Thermal Emission from Nonspherical Carbon Particles. *J.Aerosol Sci.* **2009**, *40*, 790–801.

13. Van De Hulst, H. C. *Light Scattering by Small Particles*; John Willey Press: New York, 1957.

14. Bohren, C. F.; Huffman, D. *Absorption and Scattering of Light by Small Particles*; John Wiley Press: New York, 1983.

15. Filippov, A. V.; Markus, M. W.; Roth, P. In-situ Characterization of Ultrafine Particles by Laser-induced Incandescence: Sizing and Particle Structure Determination. *J. Aerosol Sci.* **1999**, *30* (1), 71–87.

16. Filippov, A. V.; Roth, P. Laser-induced Incandescence Method for Ultrafine Particle Sizing. *J. Aerosol Sci.* **1996**, 27 (1), s699–s700.

17. Williams, M.; Loyalka, S. *Aerosol Science: Theory and Practice*; Pergamon Press: Oxford, 1991.

18. Carslaw, H. S.; Jaeger, J. C. *Conduction of Heat in Solids*; Oxford Press: Oxford, 1959.

19. Pan, Y.; Bowersett, J.; Hill, S.; Pinnick, R.; Chang, R. *Nozzles for Focusing Aerosol Particles*; ARL-TR-5026; U.S. Army Research Laboratory: Adelphi, MD, Oct. 2009.

20. Pan, Y.; Hartings, J.; Pinnick, R.; Hill, S.; Chang, R. Single-particle Fluorescence Spectrometer for Ambient Aerosols. *Aerosol Sci. Tech.* **2003**, *37* (8), 628–639.

21. Davis, E. J. A History of Single Particle Levitation. *Aerosol Sci. Tech.* **2007**, *26* (3), 212–254.

22. Ashkin, A. Acceleration and Trapping of Particles by Radiative Pressure. *Phys. Rev. Lett* **1970**, *24* (4), 156–159.

23. Huisken, J.; Stelzer, E. Optical Levitation of Absorbing Particles with a Nominally Gaussian Laser Beam. *Opt. Lett.* **2002**, *2* (14), 1223–1225.

24. Shvedov, V. G.; Hnatovsky, C.; Rode, A.; Krolikowski, W. Robust Trapping and Manipulation of Airborne Particles with a Bottle Beam. *Opt. Exp.* **2011**, *19* (18).

25. Shvedov, V. G.; Desyatnikov, A. S.; Rode, A. V. Optical Vortex Beams for Trapping and Transport of Particles in Air. *Appl. Phys. A.* **2010**, *100*, 327–331.

26. Pan, Yong-Le; Hill, Steven C. *Raman Spectra of Individual Airborne Particles*; submitted Dec. 2011, ARL-DRI Final Report.

27. Hybl, J. D.; Tysk, S.; Berry, S.; Jordan, M. Laser-induced Fluorescence-cued, Laser-induced Breakdown Spectroscopy Biological-agent Detection. *Appl. Opt.* **2006**, *45* (34), 8806–8814.

List of Symbols, Abbreviations, and Acronyms

BG	*bacillus subtilis*
BW	biological warfare
DAQ	data acquisition
DoD	Department of Defense
FOV	field of view
HeNe	helium-neon
LN2	liquid nitrogen
MCT	mercury cadmium telluride
NA	numeric aperture
Nd:YAG	neodymium-doped yttrium aluminum garnet
NEP	noise equivalent power
PMTs	photo-multiplier tubes
S/N	signal to noise
SPTES	single particle thermal emission spectroscopy

NO. OF COPIES	ORGANIZATION
1 ELEC	ADMNSTR DEFNS TECHL INFO CTR ATTN DTIC OCP 8725 JOHN J KINGMAN RD STE 0944 FT BELVOIR VA 22060-6218
6	US ARMY RSRCH LAB ATTN IMNE ALC HRR MAIL & RECORDS MGMT ATTN RDRL CIO LL TECHL LIB ATTN RDRL CIO LT TECHL PUB ATTN RDRL CIE S KRISTAN P. GURTON MELVIN FELTON YONGLE PAN ADELPHI MD 20783-1197

INTENTIONALLY LEFT BLANK.